Polymorphism of a polymer pre-cursor: Metastable glycolide polymorph recovered via large scale high-pressure experiments

Electronic Supplementary Information

Ian B. Hutchison[a], Amit, Delori[a], Xiao Wang[b], Konstantin V. Kamenev[b], Andrew J. Urquhart[c], Iain D. H. Oswald[a]

[a]Strathclyde Institute of Pharmacy and Biomedical Sciences, University of Strathclyde, 161 Cathedral Street, Glasgow, G4 0RE, UK. E-mail: ian.hutchison@strath.ac.uk; iain.oswald@strath.ac.uk
[b]Centre for Science at Extreme Conditions and School of Engineering, University of Edinburgh, Erskine Williams Building, The King's Buildings, Mayfield Road, Edinburgh, EH9 3FD, UK.
[c]Department of Micro- and Nanotechnology Colloids and Biological Interfaces, Building 423, 2800 Kgs. Lyngby, Denmark.

Contents

Experimental

Materials used
Raman Spectroscopy
Single Crystal Diffraction
Large volume press experiments
Phase Identification – X-ray Powder diffraction
Diamond Anvil Cell Experiments
Conformational analysis
PIXEL calculations

Comparison of Forms 1 and 2 of glycolide

References

EXPERIMENTAL

Materials Used

Glycolide was purchased from Sigma-Aldrich, and was recrystallized (where stated) from acetone. In any case where a pressure-transmitting medium was present, petroleum ether (40-60) was used.

Raman Spectroscopy

Raman spectra were collected on a ThermoScientific DXR Raman microscope fitted with a 532 nm laser and an extended range grating; spectra were analysed using OMNIC 8.0 software.

Single Crystal X-ray Diffraction

Refinement

X-ray diffraction intensities were collected using a Bruker Apex II diffractometer with an Incotec IμS microsource (λ=0.71073 Å). The data were reduced using SAINT within Bruker's APEX2 software and absorption corrections applied using SADABS.[1] The crystal structures were solved by direct methods (SIR92),[2] and refined against F^2 using Crystals.[3] All non-H atoms were refined anisotropically and the hydrogen atoms were geometrically placed and allowed to ride on their parent atoms. The model for Form 1 refined without any complications but the model for Form 2 was more complex. Due to the position of the molecule with respect to the inversion centre the initial model was planar and gave a suitable model with an R-factor ~4%. The thermal parameters for the oxygen atoms were observed to be larger than their neighbours when refined in the planar model indicating that there was disorder present in the crystal structure. The disordered model was created by splitting the oxygen atoms into two and refining them with distance (taken from Form 1), thermal and vibrational similarity restraints. The inversion centre dictates that the molecule is centrosymmetric however it is our belief that whilst the data suggest centrosymmetry the actual model possesses one molecule containing O10, O30, O31' and O10', while the other molecule contains O11, O31, O10' and O30'; the carbon and hydrogen atoms are the same in both molecules. Our reasoning for this is that we only required modest pressures to change the conformation and so it is unlikely that the molecule has moved over the planar transition state (70 kJ mol^{-1} higher in energy than Form 1) into the chair conformation. For comparison, P. A. Wood *et al.* observed high pressure polymorphism in L-serine in which a conformational change of 40 kJ mol^{-1} required a pressure of between 4.5 GPa and 5.2 GPa to be applied.[4] However, the molecular rearrangement in serine required a change in hydrogen bonding which may account for the greater pressure required. The crystallographic data can be found in Table S1.

Table S1 – Crystallographic data for Forms 1 and 2 of glycolide collected at ambient temperature and pressure.

	Form 1	Form 2
Crystal data		
Crystal system, space group	Monoclinic, $P2_1/n$	Orthorhombic, *Pbca*
Temperature (K)	296	293
a, b, c (Å)	6.7039 (2), 14.9481 (4), 9.6177 (2)	5.2399 (2), 7.4388 (3), 11.7763 (4)
α, β, γ (°)	90, 98.9365 (18), 90	90, 90, 90
V (Å^3)	952.10 (2)	459.02 (2)
Z	8	4
μ (mm^{-1})	0.15	0.16
Density (Mg/m^3)	1.619	1.680
Crystal size (mm)	0.50 × 0.20 × 0.20	0.42 × 0.35 × 0.21
Data collection		
$T_{\min}$, $T_{\max}$	0.85, 0.97	0.69, 0.97
No. of measured, independent and observed [$I > 2.0\sigma(I)$] reflections	9333, 2092, 1879	7121, 470, 456
R_{int}	0.027	0.036
$(\sin \theta/\lambda)_{\max}$ (Å^{-1})	0.641	0.625
Refinement		
$R[F^2 > 2\sigma(F^2)]$, $wR(F^2)$, S	0.035, 0.085, 1.06	0.042, 0.093, 0.96
No. of reflections	2075	470
No. of parameters	146	55
No. of restraints	0	38
$\Delta\rangle_{\max}$, $\Delta\rangle_{\min}$ (e Å^{-3})	0.19, -0.16	0.14, -0.19

CheckCIF statements

Form 1

912_ALERT_4_C Missing # of FCF Reflections Above STh/L= 0.600 9

The data are 99.9% to ACTA minimum resolution.

Resolution & Completeness Statistics (Cumulative and Friedel Pairs Averaged)

```
Theta sin(th)/Lambda Complete  Expected Measured  Missing
----------------------------------------------------------------------------
 20.82    0.500    0.999       1003    1002      1
 23.01    0.550    0.998       1333    1331      2
 25.24    0.600    0.999       1712    1711      1
------------------------------------------------------------ ACTA Min. Res. ---
 27.11    0.641    0.995       2102    2092     10
```

```
128_ALERT_4_G Alternate Setting of Space-group P21/c  .......     P21/n
152_ALERT_1_G The Supplied and Calc. Volume s.u. Differ by ...        2 Units
432_ALERT_2_G Short Inter X...Y Contact  O4     ..  C7      ..       2.94 Ang.
760_ALERT_1_G CIF Contains no Torsion Angles ................         ?
808_ALERT_5_G No Parseable SHELXL Style Weighting Scheme Found         !
929_ALERT_5_G No Weight Pars,Obs and Calc R1,wR2,S not checked          !
960_ALERT_3_G Number of Intensities with I .LT. - 2*sig(I) ..          7
```

Noted, no action taken

Form 2

```
088_ALERT_3_C Poor Data / Parameter Ratio ...................       8.55
910_ALERT_3_C Missing # of FCF Reflections Below Th(Min) .....          1
912_ALERT_4_C Missing # of FCF Reflections Above STh/L=  0.600          2
313_ALERT_2_C Oxygen with three covalent bonds (rare) ........       O30
313_ALERT_2_C Oxygen with three covalent bonds (rare) ........       O31
301_ALERT_3_G Note: Main Residue  Disorder ..................        50 Perc.
432_ALERT_2_G Short Inter X...Y Contact  O30    ..  C2      ..       2.96 Ang.
432_ALERT_2_G Short Inter X...Y Contact  O31    ..  C2      ..       3.01 Ang.
811_ALERT_5_G No ADDSYM Analysis: Too Many Excluded Atoms ....          !
860_ALERT_3_G Note: Number of Least-Squares Restraints .......        38
```

The model is disordered and therefore parameters for both components are required. The data are 99.8 % complete to the ACTA min. resolution. The contacts may be a little close but these will be artefacts of the disorder.

Resolution & Completeness Statistics (Cumulative and Friedel Pairs Averaged)

```
Theta sin(th)/Lambda Complete  Expected Measured  Missing
----------------------------------------------------------------------------
 20.82    0.500    0.996        236     235      1
 23.01    0.550    0.994        317     315      2
 25.24    0.600    0.998        415     414      1
------------------------------------------------------------ ACTA Min. Res. ---
 26.39    0.625    0.994        473     470      3
```

```
199_ALERT_1_G Check the Reported _cell_measurement_temperature        293 K
200_ALERT_1_G Check the Reported   _diffrn_ambient_temperature        293 K
```

The temperature of data collection was 293K

152_ALERT_1_C The Supplied and Calc. Volume s.u. Differ by ... 14 Units
760_ALERT_1_G CIF Contains no Torsion Angles .... ?
808_ALERT_5_G No Parseable SHELXL Style Weighting Scheme Found !
929_ALERT_5_G No Weight Pars,Obs and Calc R1,wR2,S not checked !

Noted, no action taken.

Large Volume Press Experiments

Design and Manufacture of the Large Volume Hydraulic Press

The cross-sectional view of the pressure cell with some key dimensions is shown in Figure ES1. The key component of the cell is its body made from BERYLCO-25 alloy with the yield strength of 1.4 GPa and machined as a cylinder opened from both ends. The inner diameter of the bore made inside the body of the cell is 10 mm. This is produced with the view to accommodate standard sample PTFE capsule to prevent potential contamination issue if the sample is expected to react with the cell material. The outer diameter of the body of the cell is 35 mm. Calculations conducted by using finite element analysis and experimental testing show that the cell can safely reach the pressure of 0.8 GPa.

The second most important part of the pressure cell is the piston which slides in the bore of the cell and is used for applying pressure to the sample. The piston is also made of BERYLCO-25, and has a copper seal which prevents the capsule from being extruded and prevents the liquid sample from leaking out. In Figure S1 the piston is shown in its initial position. At the beginning of the experiment, the cell can accommodate approximately 2.8 mL of the sample in the capsule (10 mm diameter, 64 mm long)

The pressure in the cell is generated in a hydraulic press. It is transmitted to the piston through a tungsten carbide (WC) pusher and measured by the pressure gauge of the press. The attainable pressure inside the cell was calibrated by comparing the pressure on the gauge of the hydraulic press during loading and comparing it with the results generated by finite-element method. Once the required pressure is achieved the retaining nut is rotated to lock the pressure inside the cell. The spacer between the pusher and the piston acts to prevent the twisting torque on the piston from the retaining nut. The spacer and the retaining nut are made from BERYLCO-25 alloy. Once the pressure inside the cell is locked the load in the hydraulic press can be released and the pressure can be retained for the reaction to take place.

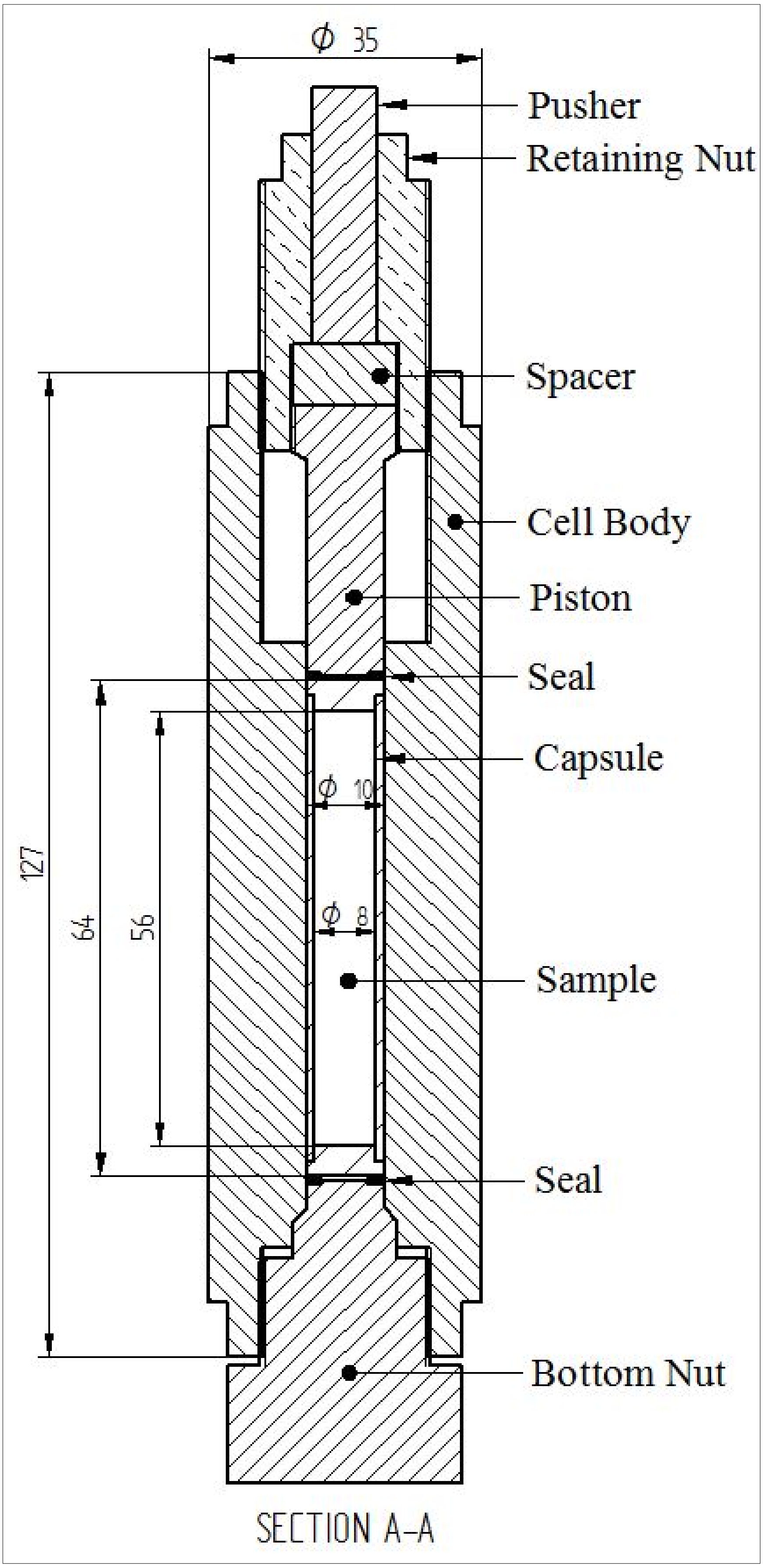

Figure S1 – Design of the large volume press. Measurements are given in millimetres.

Experimental

Four samples were loaded into the large volume press. These four samples are herein labelled LVP1, LVP2, LVP3 and LVP 4.

Samples of glycolide (1.2g – 1.5g) were placed in the PTFE capsules, which were sealed at one end with PTFE caps and PTFE tape. The remaining volume of the capsule was filled with petroleum ether and the capsule sealed at the open end in the same way. For experiments LVP1-3 the capsule was loaded into the cell, and a load of 5.5 tns (0.64 GPa) applied for a period of 24 hours. For experiment LVP4, the sample was ground before putting into the press and the pressure was maintained at 4.5 tns (0.54 GPa) for a period of 54 hours. The LVP1 loading was analysed using Raman spectroscopy and observed to be the high-pressure form. A portion of the recovered material was used to seed crystal growth from a saturated solution of glycolide in acetone.

Phase Identification – X-ray Powder diffraction

Ambient Pressure

The powder produced from the first large volume press was not analysed via X-ray powder diffraction but only the second, third and fourth attempts. A small quantity of (1 - 50 mg) of powder, directly taken from the press without grinding, was analyzed using transmission foil XRPD data collected on a Bruker AXS D8-Advance transmission diffractometer equipped with θ/θ geometry, primary monochromated radiation (Cu-Kα_1 λ = 1.54056 Å), a Bruker Vantec 1D position sensitive detector (PSD) and an automated multi-position *x-y* sample stage.[5] Samples were mounted on a 28 position sample plate supported on a polyimide (Kapton, 7.5 µm thickness) film. Data were collected from each sample in the range 4 – 35° 2θ with a 0.015° 2θ step size and 45 sec. step^{-1} count time. Figure S2-4 show the X-ray powder diffraction patterns of the solid recovered from the large volume press experiments (LVP2-4). In LVP2, the conversion to From 2 was not complete but we were able to Pawley fit both unit cells of Form 1 and 2 to the pattern confirming that the recrystallised sample that we observed was indeed the form produced at high pressure.[6] There are other peaks which cannot be attributed to either polymorph of glycolide, or to glycolic acid, suggesting the possible low-level presence of some impurities.

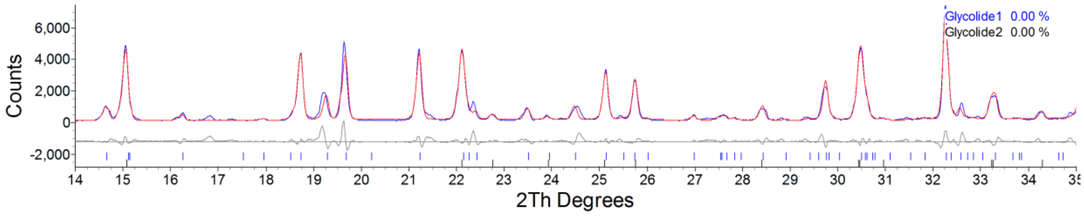

Fig S2 – Pawley fit of the recovered material from LVP2 with Forms 1 and 2 of glycolide.

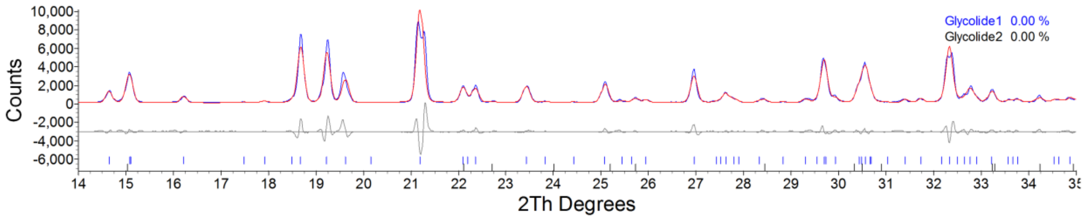

Fig S3 – Pawley fit of the recovered material from LVP3 with Forms 1 and 2 of glycolide.

The final large volume press experiment, LVP4, was carried out in order to determine if particle size was an important factor in the extent of conversion from Form 1 to Form 2. Glycolide was gently ground to ensure small particle size before being loaded into the large volume press. Having previously obtained Form 2 at 0.12 GPa in a DAC experiment, this sample was prepared in the same way and then taken to 0.54 GPa. The sample was left at high pressure for 54 hours before decompression, drying over a Buchner funnel and analysis by PXRD. The observed pattern, shown in Fig S4, shows that the resulting powder was pure Form 1.

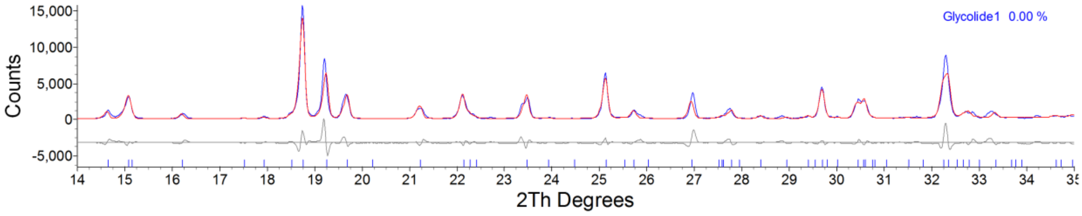

Fig S4 – Pawley fit of the powder recovered from experiment LVP4 against the unit cell parameters of Form 1.

High-pressure powder diffraction

Powder diffraction at high pressure was performed on a powder loaded into a diamond anvil cell with petroleum ether as the pressure transmitting medium. The DAC was aligned using normal high pressure single crystal diffraction procedures. Data were collected using Mo-Kα radiation (0.71073 Å) and the data analysed in the Phase ID module found in the APEX2 software package. The data were collected at 0.12 GPa, with a single exposure of 600 seconds covering a scan width of 20°. Pawley refinement was performed using TOPAS academic.[6] Figure 4 (main paper) shows the X-ray powder diffraction image of glycolide in the DAC at 0.12 GPa. The Pawley fit was carried out using the unit cell parameters obtained via single crystal diffraction of a crystal of Form 2.

Diamond Anvil Cell Experiments

A Merrill-Bassett diamond anvil cell (DAC) with 600 μm culet diamonds on tungsten carbide backing disks was used.[7,8] A 250 μm thick tungsten foil gasket was indented to ~100 μm, and a 300 μm hole drilled in the indented portion of the gasket to create a sample chamber. A small piece of ruby was placed in the sample chamber to allow in-situ pressure measurement via the Ruby fluorescence technique.[9]

During the initial DAC experiment, a single crystal of glycolide (recrystallized from acetone) was placed in a DAC along with a ruby sphere and petroleum ether as a pressure transmitting medium. A small portion of the single crystal was crushed during the loading procedure, and Raman data were collected on both the powdered and single crystal portions. It was noted that the Raman pattern of the crushed (i.e. powdered) sample of glycolide exhibited some changes not seen in the single crystal portion.

Conformational Analysis

The analysis of the different molecular conformations were performed using Gaussian09W[10] through Materials Studio interface. The molecular geometries were taken from the crystal structures. The analysis of Form 1 was relatively straightforward, taking the molecular conformations from the crystal structure. In the case of the conformation of Form 2 we constructed a new model using the refined positions of the disordered components. We took the position of O11 and the position for the symmetry related atom of O10, O10' and repeated this for the other two oxygen atoms, O30 and O31'. This provided us with a model that we believe to be the true model as opposed to the model imposed on us by symmetry. The model we took as being the true model contained O11, O31, O10' and O30'. Single point energy calculations were performed using Density Functional Theory with a 6-31G* Basis Set and B3LYP exchange correlation.

PIXEL calculations

PIXEL calculations, as incorporated in the CLP suite of programs, were performed on the two crystal structures to determine the intermolecular energies between the two molecules. The crystal structure of Form 1 formed the basis of the calculation of intermolecular interactions for this form. In Form 2, however, PIXEL is unable to calculate for crystal structures with Z'<1. This problem worked to our advantage as it meant that we were able to use the molecular conformation which we believe to be the true conformation. Similar to the conformational analysis we used the coordinates from the refined model but instead of using symmetry-equivalent atoms, we used the unrelated O atoms to complete the molecule. From this the molecular electron densities were calculated using Gaussian09W with the MP2/6-31G** basis set.[10]

Interaction energies

Figures S5 and S6 show the most significant interactions in Form 1 and Form 2, respectively, where Interaction 1 is the strongest observed in the crystal structure. Table S2 details the breakdown of energies with respect to coulombic, polarisation, dispersion and repulsion forces as calculated using PIXELC module of the CLP suite of programs.[11] In the construction of Figure S6 the disorder model was used due to the imposition of the inversion symmetry. We stress that the boat conformation was used in the calculation of the energies. The diagrams are the best approximation.

The most notable interaction from Form 1 is the molecular interaction that encompasses an anti-parallel C=O dimer (Int. 1). Although PIXEL gives molecule-molecule energies an important contribution to this energy is the dispersion component which is known to contribute to carbonyl-carbonyl interactions. These interactions have been shown by Allen *et al.* to be comparable with medium strength hydrogen bonds.[12] Interestingly, despite the strength of these interactions Form 2 does not possess any such interactions. Previous work by our group on acrylic acid showed that both low pressure and high pressure phases possessed these interactions.[13]

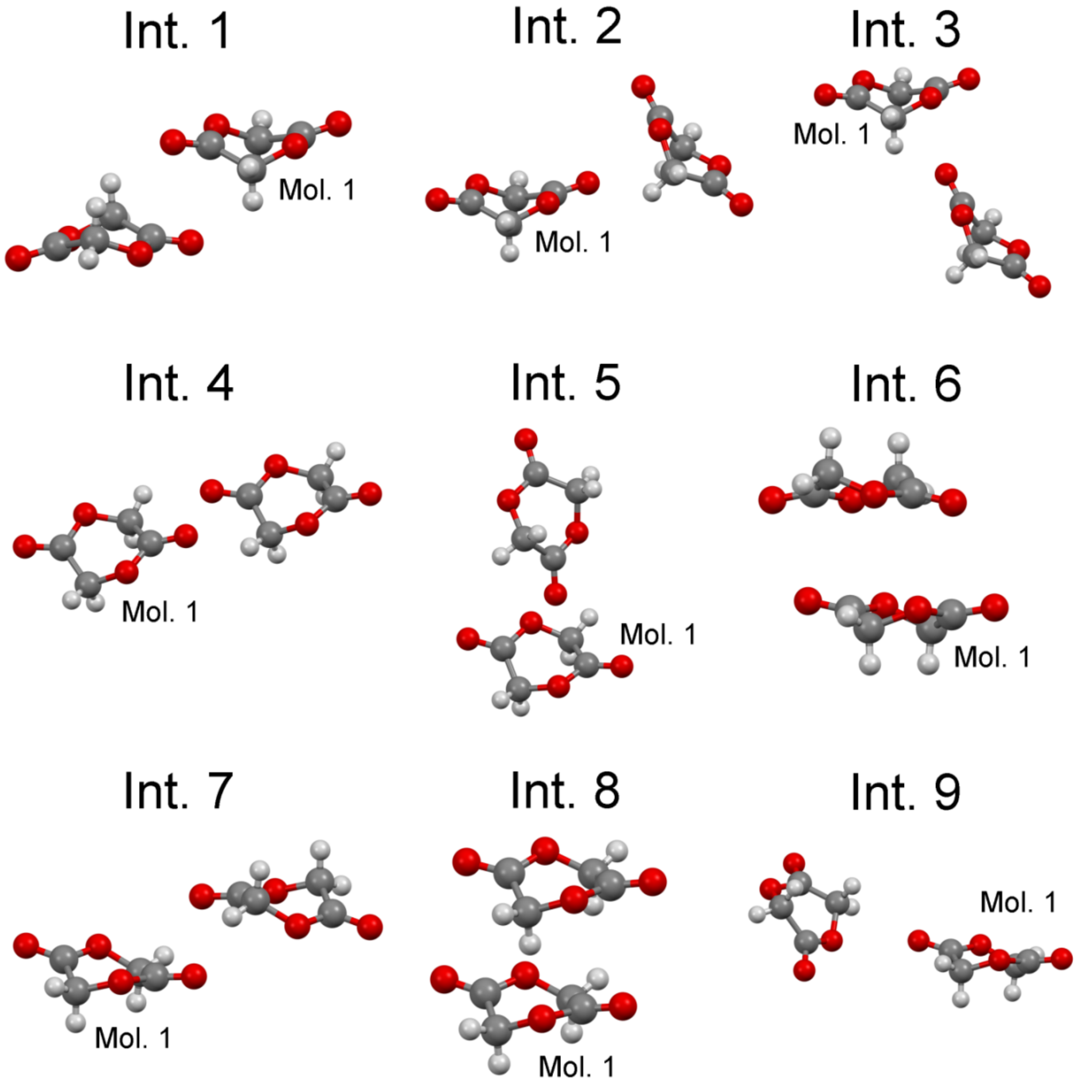

Figure S5: The nine most prominent interactions in Form 1 of glycolide ranging from -10.5 to -34.9 kJmol^{-1}. Table S2 shows the interaction energies.

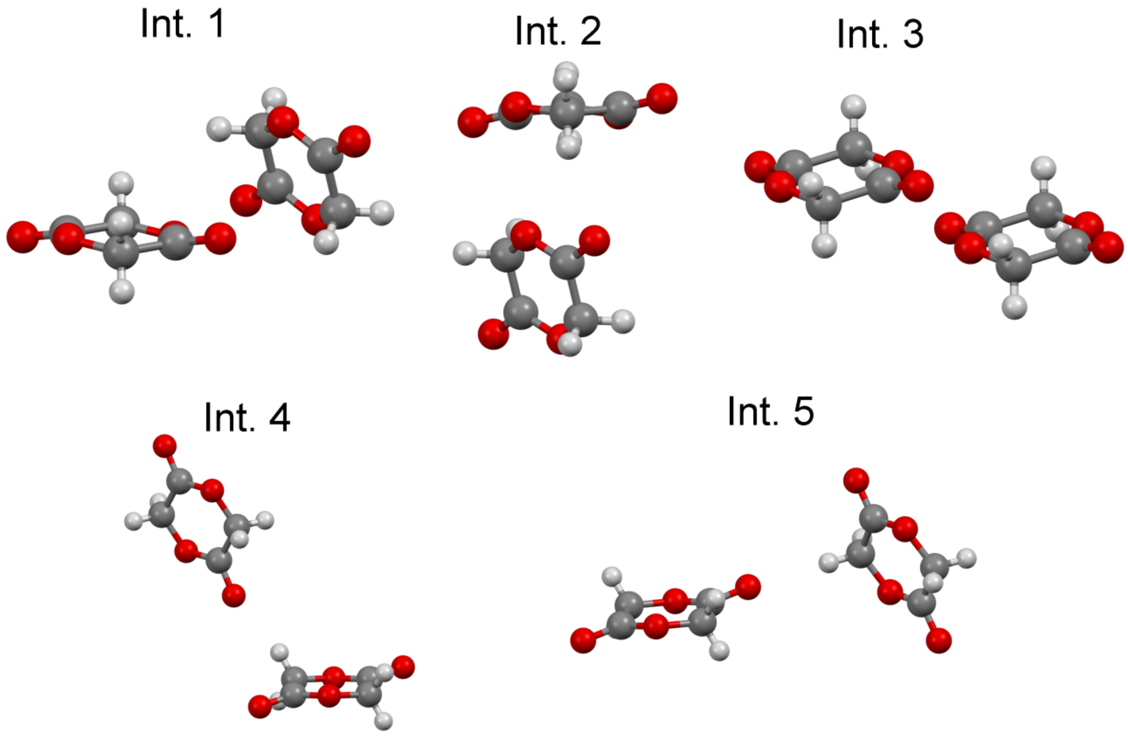

Figure S6: The five most prominent interactions in Form 1 of glycolide ranging from -9.0 to -25.0 kJmol^{-1}. Table S2 shows the interaction energies.

Tables S2: The interactions energies in kJmol^{-1} for Forms 1 and 2 of glycolide as calculated by PIXELC.

Interaction	C_m-C_m dist. ^{a} (Å)	E_{coul} (kJmol^{-1})	E_{pol} (kJmol^{-1})	E_{disp} (kJmol^{-1})	E_{rep} (kJmol^{-1})	E_{tot} (kJmol^{-1})
Form 1						
1	5.219	-27.5	-5.9	-15.4	13.9	-34.9
2	5.725	-18.7	-4.6	-10.2	12.4	-21.1
3	5.613	-19.0	-5.1	-11.0	15.9	-19.2
4	6.415	-11.1	-2.4	-7.2	5.3	-15.4
5	5.897	-9.3	-1.9	-7.8	3.8	-15.2
6	3.800	-5.2	-2.6	-16.2	9.6	-14.3
7	5.935	-10.0	-4.9	-11.6	14.4	-12.1
8	5.596	-7.8	-2.0	-8.2	6.3	-11.7
9	6.616	-9.1	-1.9	-5.1	5.6	-10.5
Form 2						
1	4.546	-19.0	-5.9	-17.3	17.3	-25.0
2	4.553	-15.1	-4.8	-16.0	12.6	-23.3
3	5.240	-8.0	-1.4	-7.0	1.9	-14.5
4	6.976	-6.9	-1.2	-3.2	2.0	-9.3
5	6.953	-7.3	-1.5	-3.8	3.5	-9.0

^{a}Cm denotes the centre of mass.

References

1. G. M. Sheldrick, *Univ. Gottingen, Ger. Bruker AXS Madison, Wisconsin, USA*, 2001.

2. A. Altomare, G. Cascarano, C. Giacovazzo, A. Guagliardi, M. C. Burla, G. Polidori, and M. Camalli, *J. Appl. Crystallogr.*, 1994, **27**, 435.

3. P. W. Betteridge, J. R. Carruthers, R. I. Cooper, K. Prout, and D. J. Watkin, *J. Appl. Crystallogr.*, 2003, **36**, 1487.

4. P. A. Wood, D. Francis, W. G. Marshall, S. A. Moggach, S. Parsons, E. Pidcock, and A. L. Rohl, *CrystEngComm*, 2008, **10**, 1154–1166.

5. A. J. Florence, B. Baumgartner, C. Weston, N. Shankland, A. R. Kennedy, K. Shankland, and W. I. F. David, *J. Pharm. Sci.*, 2003, **92**, 1930–1938.

6. A. Coelho, *TOPAS – Acad. Gen. Profile Struct. Anal. Softw. Powder Diffr. Data*, 2012.

7. S. A. Moggach, D. R. Allan, S. Parsons, and J. E. Warren, *J. Appl. Crystallogr.*, 2008, **41**, 249–251.

8. L. Merrill and W. A. Bassett, *Rev. Sci. Instrum.*, 1974, **45**, 290–294.

9. G. J. Piermarini, S. Block, J. D. Barnett, and R. A. Forman, *J. Appl. Phys.*, 1975, **46**, 2774–2780.

10. M. J. Frisch, G. W. Trucks, H. B. Schlegel, G. E. Scuseria, M. A. Robb, J. R. Cheeseman, G. Scalmani, V. Barone, B. Mennucci, G. A. Petersson, H. Nakatsuji, M. Caricato, X. Li, H. P. Hratchian, A. F. Izmaylov, J. Bloino, G. Zheng, J. L. Sonnenberg, M. Hada, M. Ehara, K. Toyota, R. Fukuda, J. Hasegawa, M. Ishida, T. Nakajima, Y. Honda, O. Kitao, H. Nakai, T. Vreven, J. A. Montgomery, J. E. Peralta, F. Ogliaro, M. Bearpark, J. J. Heyd, E. Brothers, K. N. Kudin, V. N. Staroverov, R. Kobayashi, J. Normand, K. Raghavachari, A. Rendell, J. C. Burant, S. S. Iyengar, J. Tomasi, M. Cossi, N. Rega, J. M. Millam, M. Klene, J. E. Knox, J. B. Cross, V. Bakken, C. Adamo, J. Jaramillo, R. Gomperts, R. E. Stratmann, O. Yazyev, A. J. Austin, R. Cammi, C. Pomelli, J. W. Ochterski, R. L. Martin, K. Morokuma, V. G. Zakrzewski, G. A. Voth, P. Salvador, J. J. Dannenberg, S. Dapprich, A. D. Daniels, Farkas, J. B. Foresman, J. V Ortiz, J. Cioslowski, and D. J. Fox, 2009.

11. A. Gavezzotti, *J. Phys. Chem. B*, 2003, **107**, 2344–2353.

12. F. H. Allen, C. A. Baalham, J. P. M. Lommerse, and P. R. Raithby, *Acta Crystallogr. Sect. B-Structural Sci.*, 1998, **54**, 320–329.

13. B. F. Johnston, W. G. Marshall, S. Parsons, A. J. Urquhart, and I. D. H. Oswald, *J. Phys. Chem. B*, 2014, **118**, 4044–51.